mAbs 6:6, 1540–1550; November/December 2014; Published with license by Taylor & Francis Group, LLC

Remediating agitation-induced antibody aggregation by eradicating exposed hydrophobic motifs

Rutilio H Clark[1,*], Ramil F Latypov[2], Cyr De Imus[1], Jane Carter[1], Zien Wilson[1], Kathy Manchulenko[1], Michael E Brown[1], and Randal R Ketchem[1]

[1]Department of Therapeutic Discovery; Amgen Inc.; Thousand Oaks, CA USA; [2]Department of Drug Product Development; Amgen Inc.; Thousand Oaks, CA USA

Keywords: agitation, aggregation, antibody, computational, engineering, in silico, modeling, stability, thermal

Abbreviations: SAP, spatial aggregation propensity; RAP, relative aggregation propensity; mAb, monoclonal antibody; IgG, immunoglobulin G; Fv, variable fragment; Fab, fragment antigen-binding; CDR, complementary-determining regions

Therapeutic antibodies must encompass drug product suitable attributes to be commercially marketed. An undesirable antibody characteristic is the propensity to aggregate. Although there are computational algorithms that predict the propensity of a protein to aggregate from sequence information alone, few consider the relevance of the native structure. The Spatial Aggregation Propensity (SAP) algorithm developed by Chennamsetty et. al. incorporates structural and sequence information to identify motifs that contribute to protein aggregation. We have utilized the algorithm to design variants of a highly aggregation prone IgG_2. All variants were tested in a variety of high-throughput, small-scale assays to assess the utility of the method described herein. Many variants exhibited improved aggregation stability whether induced by agitation or thermal stress while still retaining bioactivity.

Introduction

The value of protein therapeutics in human medicine is well known. The large gains demonstrated in the marketplace are a testament to the demand for antibody medicines, which is expected to increase.[1] However, manufacturing protein therapeutics is an expensive and complicated process involving the control of many parameters. Appropriate control of these parameters is critical to producing a quality medicine. One compromise in quality that these biomolecules can experience is the phenomena of protein aggregation.[2,3] Aggregation is considered an undesirable phenomenon that leads to a decrease in available efficacious product, potential immunogenicity in the patient and a host of other potential issues.[4,5] Protein aggregation can occur at any point during or after manufacturing. Physical stresses on the protein post manufacturing such as elevated temperatures or agitation on shipping (transportation) can induce aggregation.[6] The extent that a protein can withstand a particular stress is related to its stability to that stress. An environment can be found to stabilize the protein, such as through formulation screening. However, it is also possible to engineer the protein to withstand a stress, conferring a specific type of stability.[7]

We have encountered an IgG2 (mAb_A) that exhibited good solubility up to 70 mg/mL, but when agitation stressed, experienced severe aggregation. In silico homology modeling indicated a large amount of exposed hydrophobicity with respect to hydrophilicity in the variable fragment (Fv). The absolute amount of exposed hydrophobic surface area was similar to many other in-house Fv domains, but the absolute amount of exposed hydrophilicity was lower than typical for in-house Fv domains. For instance, the hydrophobic surface area for all Fvs in this therapeutic project was within 4% of each other (with an average of 5665 square ångstroms). The hydrophilic surface area for all Fvs was within 1.3% of each other except for the Fv of mAb_A. The hydrophilic surface area of the mAb_A Fv was 3226 square ångstroms whereas the average for the other Fvs was 4815 square ångstroms. Additionally, the exposed hydrophobicity was arranged such that large patches were formed on the surface of the mAb_A Fv. We hypothesized that the large hydrophobic patches in the Fv were responsible for agitation instability of the IgG2. The lack of surface hydrophilicity and presence of large hydrophobic patches needed to be addressed simultaneously. One strategy for disrupting the hydrophobic patches is by inserting charged or hydrophilic, or less hydrophobic, residues within

*Correspondence to: Rutilio H Clark; Emails: rutilioc@amgen.com, rutilioc@gmail.com

Submitted: 07/31/2014; Revised: 08/25/2014; Accepted: 08/26/2014

http://dx.doi.org/10.4161/mabs.36252

the patches or by simply deleting the offending hydrophobic residues. This strategy is uncommon for this type of situation. Considering that the majority of the exposed hydrophobicity was in the complementarity-determining regions (CDRs), we suspected that the paratope structure would be too drastically modified using those methods and therefore changes such as these would be detrimental to antibody function. Therefore, instead of merely inserting or deleting residues, we chose the strategy of attempting to retain the majority of the tertiary structure by substituting offending hydrophobic residues with either charged or hydrophilic or less hydrophobic residues.

The spatial aggregation propensity (SAP) algorithm developed in Bernhardt Trout's laboratory at Massachusetts Institute of Technology[8] identifies and quantitatively calculates the degree of exposed hydrophobic motifs. The SAP algorithm, as part of the Accelrys Discovery Studio Suite (San Diego, CA), identified many residues and motifs that could be relevant to conferring aggregation instability in mAb_A. We selected certain sites with high SAP scores for site-directed mutagenesis. The type of residue substitution performed at each position was guided by utilizing a somewhat homologous IgG2 (mAb_B) that bound to the same target as mAb_A. Antibody 'B' was found to be much more agitation stable in a small-scale relative aggregation propensity (RAP) assay we developed in-house. The high throughput RAP assay allowed us to efficiently test the stability of many variants by monitoring antibody loss post agitation or thermal stress. Not only was mAb_B less aggregation prone than mAb_A, it also exhibited high bioactivity to the same target as mAb_A and had the same VH1 subtype as mAb_A. Therefore, it seemed reasonable to choose it as a guide for residue substitution. The SAP algorithm indicated which residues to focus on, whereas the similar mAb_B suggested the type of substitutions for the offending mAb_A residues. Each variant was expressed as a full-length IgG2 and tested for agitation and thermal stability, target binding and biological activity.

Results

Engineered constructs

The symmetric difference set of Fv SAP motifs for mAb_A and mAb_B is shown in **Table 1**. Other SAP motifs were found in mAb_A and mAb_B but they were common in many stable Fvs we have worked with. We deduced that these common SAP motifs probably did not contribute to the aggregation observed in our assays. Although mAb_B did contain a high-scoring SAP motif, we did not observe agitation or thermal instability to the extent of mAb_B. The SAP motif in mAb_B was located in CDR3 of the VH. The SAP motifs present in mAb_A but absent in mAb_B were the focus of our engineering strategy. Amgen reference numbering is used throughout this report. Within the Fv this numbering system is based upon the AHo numbering scheme.[9]

Table 1. The symmetric difference set of Fv SAP motifs in mAb_A and mAb_B. "Central Residue" refers to the central residue of the SAP motif spatial cluster. Higher SAP motif scores indicate a greater degree of exposed local hydrophobicity and potential region for driving aggregation

Central Residue	Antibody	Motif Score
L9_VL	mAb_A	0.556
F29_VH	mAb_A	0.291
I69_VH	mAb_A	0.403
W110_VH	mAb_A	0.250
L135_VH	mAb_B	0.799

Table 2. Select SAP properties of mAb_A Fv and the engineering design. "Central" refers to the central residue of the motif spatial cluster. "Peripheral" residues are those that were within 5 Ångstroms of the high scoring central residue and also chosen for engineering. Residues with the same motif score were in the same motif

mAb_A	SAP Motif Location	Motif Score	Substitution
L9_VL	Central	0.556	D
T39_VL	Peripheral	0.21	D
F29_VH	Central	0.291	Y
I30_VH	Peripheral	0.291	T
I69_VH	Central	0.403	A, D, K, S
L80_VH	Peripheral	0.403	M
W109_VH	Peripheral	0.250	E
W110_VH	Central	0.250	D
F134_VH	Peripheral	0.250	G

The engineering strategy of the mAb_A variants is outlined in **Table 2**. Although antigen-binding fragments (Fabs) were used *in silico*, full-length mAbs were made of all constructs for assays. The 74 variants were designed combinatorially. All but one of the engineered positions was within, or proximal to, the CDRs. Only position L9_VL was CDR distant (proximal to the first β turn in framework 1). It was therefore likely that activity of the antibodies would be affected. **Figure 1** shows the locations of the engineered positions.

I69_VH was present in both mAb_A and mAb_B, but a larger aggregation propensity score was assigned to I69_VH in mAb_A than in mAb_B. The compositional environment of the I69_VH motif was similar in both mAbs except for at position VH_80. A leucine was present at that position in mAb_A, whereas a methionine existed at that position in mAb_B. The structural environment was also different where I69_VH was 65% more solvent exposed in mAb_A than in mAb_B as calculated *in silico*. To address these potential contributors to the differences in aggregation propensity between mAb-A and mAb-B, both positions were modified as described in **Table 2**. T39D_VL was included in most variants. Although the T39_VL relative aggregation propensity score was low, the corresponding residue in mAb_B was Asp, and it is known that charged residues confer stability in certain situations.[10] The remainder of the positions were substituted in a combinatorial fashion.

Transient cell expression antibody titer

Twenty-four mAb_A variants expressed at a lower level than the parent. Nine of these did not express sufficiently to be processed through all of the remaining steps from purification through analytics. No particular sequence or structural property of these low expressors could be deduced as a potential cause of low expression.

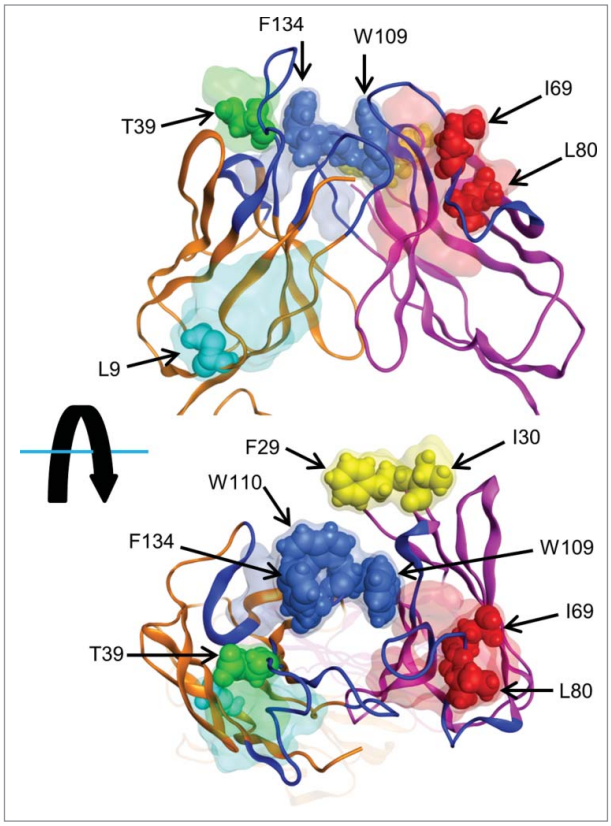

Figure 1. Locations of the engineered sites in the Fv of mAb_A. The variable light domain is rendered in orange ribbon. The variable heavy domain is rendered in magenta ribbon. The CDRs are rendered in dark blue ribbon. Only the residues rendered in CPK were substituted as described in **Table 2**. CPK Residues of the same color belong to the same SAP motif. Each SAP motif is indicated by the molecular surface of the same color to which the CPK residues belong. The upper image was rotated 90° toward the viewer to accomplish the orientation shown on the lower image where the CDRs are oriented toward the viewer.

However, it seems likely that low expression could be due to some protein instability or issues with folding. Protein thermal stability has been shown to be related to expression titer in *E. coli*[11] and mammalian expression systems.[12,13] **Figure 2B** shows this trend of increasing titer with increasing thermal stability as determined by the RAP assay. However, a strong relationship between agitation stability of the variants and expression titer was not observed (**Fig. 2A**). All variants involved substituting surface exposed residues, and it is known that charged surface residues can affect protein thermal stability[14] and aggregation.[15] By decreasing the amount of surface hydrophobicity, the probability of burying the proper hydrophobic core during intracellular folding would increase, thereby improving titer.[15,16]

Relative aggregation propensity

We utilized our high-throughput in-house method for measuring RAP.[17,19] This approach utilizes highly sensitive analytical techniques (HPLC or MS), which allow generation of stability data using only micrograms of protein. To increase reliability of the RAP data, up to 6 or more different proteins are combined into a single mixture, which is then subjected to a stress. Protein mixtures can then be resolved by cation-exchange HPLC (CEX), as illustrated in **Figure 3B**, and peak heights compared prior and post stress to estimate monomer recovery. A representative CEX column elution profile of a mixture consisting of mAb_A and mAb_B is shown in **Figure 3A**. The 3 overlaid chromatograms represent unstressed (in black) and 2 post-agitation stressed (in blue and red) aliquots from the same sample. The extent of peak height or peak area decrease from the unstressed to the stressed samples is indicative of the mAb instability for that duration of agitation of stress. The peak height decrease of mAb_B post stress relative to unstressed control is much less than for mAb_A for agitation stress (a similar rank order of stability was revealed post thermal stress; chromatogram results not shown for brevity). This indicates an increased relative stability of mAb_B compared to mAb_A under identical conditions achieved via mixing the proteins in a single container. The mAb_A variants were interrogated in the RAP assay in mixtures that included proteins with non-overlapping CEX profiles. Since all 74 variants of mAb-A could not be mixed and analyzed in a single mixture, multiple standards, including parent molecules, were included in each mixture of up to 6 mAbs total per run to ensure consistency in the stability rank order.

The agitation stability of a variant was often improved by incorporating a higher number of residue substitutions. This is shown in **Figure 4A**. No particular site consistently conferred a large improvement to stability against either agitation or thermal stress. For instance, L9_VL had the largest amount of exposed hydrophobicity based on square ångstroms and was the central residue of the highest scoring SAP motif. However, there were L9D_VL constructs that even when included with 2 other substitutions did not exhibit improved agitation stability. While referring to **Figure 4A**, it might appear that I69A_VH provided the greatest remediation benefit on a per residue basis. I69A_VH did impart approximately 40% greater agitation stability when the substitution was performed in isolation. However, the only other construct that contained the I69A_VH substitution also included 7 other changes. It is uncertain if a linear relationship would have been observed between the number of residue substitutions added to the I69A_VH construct and improved agitation stability. The agitation stability of constructs that contained 8 substitutions was too similar to assign unequal benefit to any particular substitution.

The relative agitation and thermal stability of most of the mAb_A variants engineered in this study are shown in **Figure 4B**. Since some variants did not express sufficiently to be purified, complete datasets are not available for every engineered mAb_A. The axes drawn from the parental mAb_A marker subdivide the plot into 4 sections. The variants in the lower left section demonstrated improved thermal and agitation stability compared to the parental. There were 32 variants that demonstrated this dual stability. There were 47 variants that were more agitation stable than the parent, including 2 variants that demonstrated similar agitation stability to mAb_B. These 2 variants with high agitation stability contained 8 substitutions. One variant, mAb_A_59 (L9D,T39D_VL with F29Y, I30T, W110D, F134G_VH) exhibited similar stability to mAb_B to both

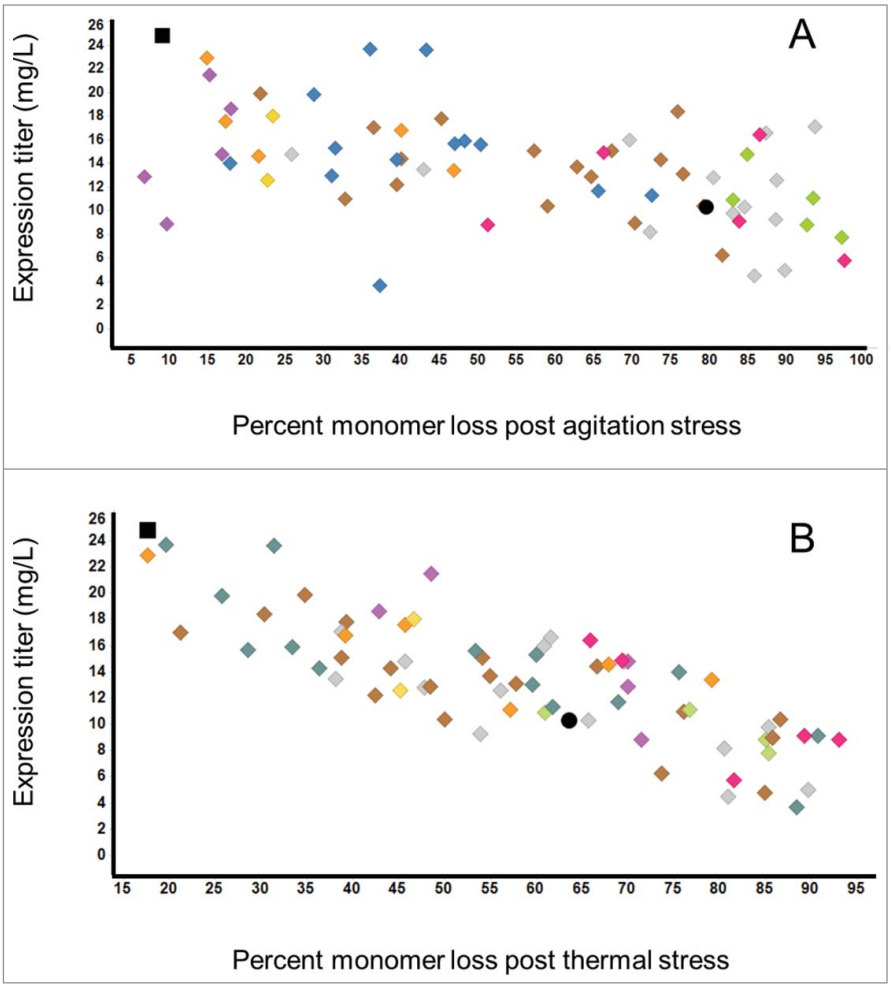

Figure 2. The relationship between transient expression antibody titer and either agitation stability (**A**) or thermal stability (**B**). Monoclonal antibody 'A' (mAb_A) is indicated by the black circle and mAb_B is indicated by the black square. The variants of antibody 'A' are designated by the diamonds. The color of the diamonds represents the quantity of substitutions as compared to antibody 'A'. Red, green, gray, brown, blue, orange, yellow and purple represents 1 through 8 substitutions in a variant, respectively. Antibody variants with improved thermal stability usually exhibited higher expression titer. The same trend was not as evident for agitation stability.

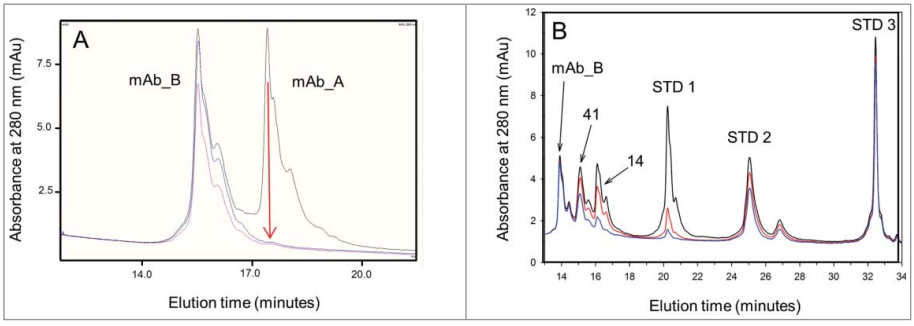

Figure 3. A cation exchange (CEX) column elution profile of the parent antibodies (**A**) and an antibody mixture (**B**). The CEX profile on the parent antibodies shown in (**A**) shows the dramatic stability difference between mAb_A and mAb_B post agitation (vortexing). The unstressed sample chromatogram is indicated by the black trace. The red and blue traces are from the same sample stressed by agitation for either 10 or 30 minutes, respectively. The decrease in peak height reflects sample loss due to protein aggregation induced by the stress. Shown in CEX profile (**B**) are 2 variants of mAb_A (14 and 41) along with the mAb_B control and 3 other stability standards (STD 1–3). Color coding in (**B**) is the same as in (**A**). Shown in this example chromatogram is mAb_A_41 with improved agitation stability over mAb_A_14, but neither exhibited agitation stability to the extent of mAb_B.

stresses. However, mAb_A_59 did not bind to the target and was not active in the NK assay. None of the variants with 8 substitutions were active in the NK assay.

Binding and activity

Variants that did not bind in the Biacore assay also did not exhibit activity in the NK assay. **Figure 5** shows all of the variants that bound in the Biacore assay. A total of 35 variants retained binding as defined by a less than 12.5 nM disassociation constant. Of the 35 variants that bound, 25 retained activity as defined by an IC50 of less than 500 pM. Of the 25 variants that were still active, 13 were also more agitation stable than the parent. Nine variants exhibiting improved thermal and agitation stability retained activity in the NK assay. The most overall stable and active variant was mAb_A_42. It contained the substitutions L9D_VL, T39D_VL and I69T_VH. The locations of these 3 sites are shown in **Figure 6**. The next 2 best candidates, considering stability and activity, were mAb_A_16 and mAb_A_48. The 4 substitutions incorporated into mAb_A_16 were T39D_VL, I69T_VH, W109E_VH and W110D_VH. The same 4 substitutions were present in mAb_A_48, but with the additional L9D_VL substitution. **Table 3** summarizes the performance of variants.

Discussion

Our primary interest in embarking on this study was to understand the utility of the SAP algorithm to remediate agitation-induced instability. There are many

bioinformatics tools that predict aggregation prone motifs exclusively from sequence information.[17] An advantage to using a primary structure-based tool is that a tertiary structure is unnecessary. However, our homology model indicated that the hydrophobic patches were not linear in sequence space but rather spatially arranged. Since we hypothesized these hydrophobic patches were relevant to aggregation instability, we were interested in applying an algorithm that utilizes structural information to predict aggregation prone motifs in mAb_A. Utilizing the SAP algorithm and a homologous antibody mAb-B as a guide, 74 variants of mAb_A were designed, cloned, expressed, purified and analyzed all at the small-scale in a high-throughput fashion.

The CEX-based methodology used here for comparing aggregation propensity of monoclonal antibodies in mixtures has been established by Chen et al. in 2010.[18] The high-throughput assay allows for the ranking of many antibodies based upon their stability without requiring large quantities of protein. Both agitation and thermal stresses induced rapid aggregation, which led to significant loss of monomer, sometimes approaching 100%.

Relative aggregation propensity experiments on parental mAb_A and mAb_B revealed instability of the former in both aggregation tests. The most stable version of mAb_A generated in this study had an agitation stability that was comparable to that of mAb_B. However, its thermal stability, while improved, had not increased to the level of mAb_B. The lack of agreement between protein stability predictions based on different stresses was previously seen.[18,19] The mechanism of thermal denaturation of proteins has been elucidated to a greater degree compared to agitation. Although agitation stress has important applications in candidate selection and formulation development in the biotech industry, detailed understanding of its effects is missing.

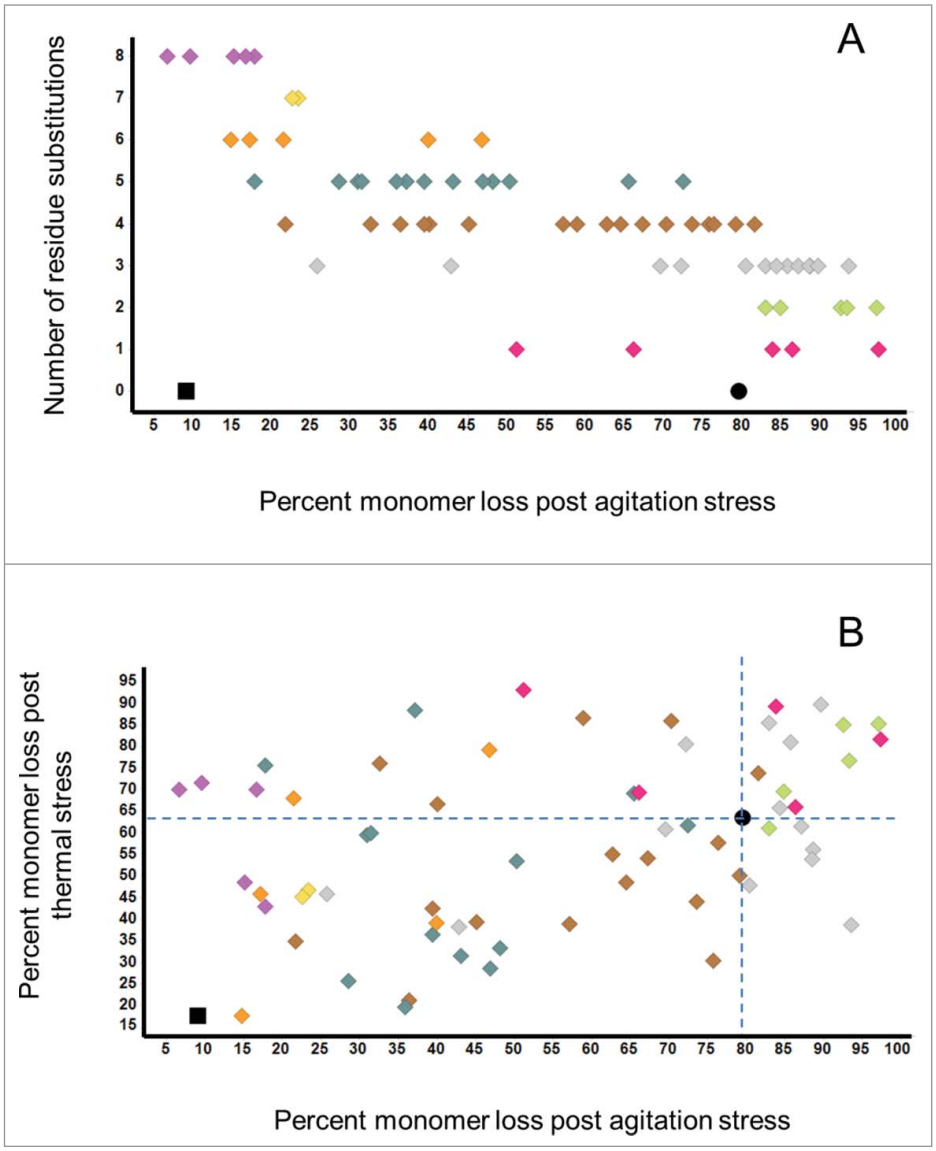

Figure 4. Agitation and thermal stability of all purified antibodies. Monoclonal antibody 'A' (mAb_A) is indicated by the black circle and mAb_B is indicated by the black square. The variants of antibody 'A' are designated by the diamonds. The color of the diamonds represents the quantity of substitutions as compared to antibody 'A'. Red, green, gray, brown, blue, orange, yellow and purple represents 1 through 8 substitutions in a variant, respectively. Plot (**A**) shows that engineered mAb_A variants with a higher number of residue substitutions often conferred improved agitation stability. However, those variants with improved agitation stability did not always exhibit improved thermal stability as shown in plot (**B**). The variants in the lower-left section of the plot did exhibit improved stability to both stresses as compared to the mAb_A parent. The quantity of substitutions indicated by the ordinate only applies to the engineered variants of mAb_A.

Our RAP results generated using mAb mixtures could potentially be affected by 2 molcular processes. First, different IgGs in a given mixture would likely compete with each other for the air-water interface. This, however, might not have had a major effect taking into account the very short time-scale at which the interface was renewed (upon vigorous vortexing) in our experiments. Second, the agitated antibodies might have denatured and aggregated concurrently, thus enabling co-precipitation. We addressed this possibility by running control experiments stressing one antibody species in isolation and in antibody mixtures. Irrespective of the presence or absence of mAb_A, mAb_B exhibited high resistance toward aggregation and did not co-precipitate. Similarly,

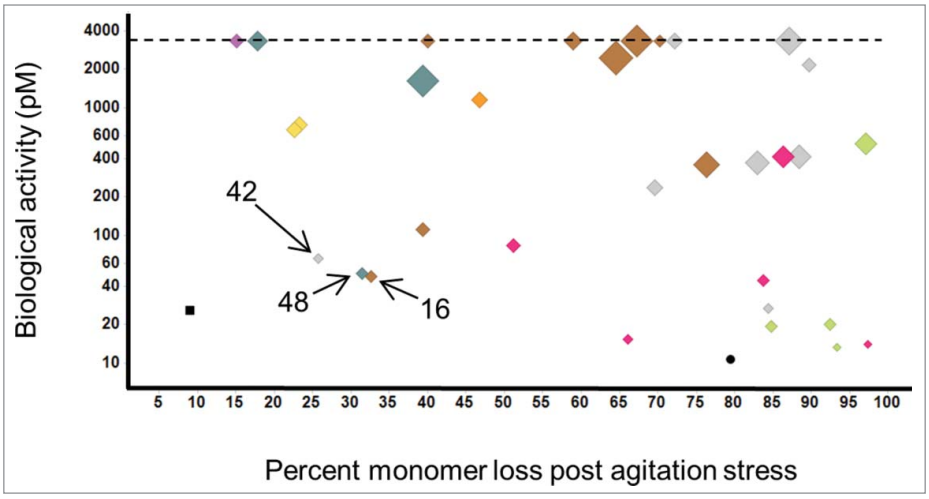

Figure 5. Antibodies that bound in the Biacore assay. The black circle represents mAb_A, the black square represents mAb_B and the mAb_A variants are represented by the diamonds. The color of the diamonds represents the number of residue substitutions as compared to the mAb_A parent (as described in previous figures). Marker size from smallest to largest indicates the binding affinity range from 0.18 nM to 12.40 nM. The dotted line is the upper limit of quantitation of the biological assay, 3.33 nM. The 3 labeled variants exhibited improved agitation stability and sub-100 pM biological activity. The only substitution they all had in common was I30T in framework 1 of the VH.

mAb_A always showed rapid loss of monomer regardless if mAb_B was present or absent. IgG standard(s) and mAb_B molecules were included in each mixture as internal controls to ensure appropriate duration and intensity of agitation. The validity of this approach for rank ordering IgGs in complex mixtures was further demonstrated in 3 separate studies.[18-20] It has been demonstrated that incorporating more residue substitutions resulted in greater agitation stability. However, activity of the antibody usually decreased as more residue substitutions were introduced due to structural or chemical changes of the paratope. Many positions were within or near the CDRs and therefore effects on binding and biological activity were to be expected. We were also interested in retaining biological activity because this is a critical component for therapeutic efficacy. The most stable variant that retained the most biological activity was mAb_A_42. **Figure 6** shows the distribution of the 3 substitutions of mAb_A_42 (I30T_HC, T39D_HC, L9D_LC). The residue positions were spatially separated around the Fv reducing the large SAP motifs. The contiguously exposed hydrophobic patches were disrupted just enough to remediate most of the agitation instability. Since these residue substitutions did not dramatically affect binding and activity, they therefore did not dramatically affect the paratope. T39D was located in a CDR_L1, whereas the others were in frameworks, although I30T_VH is probably near the paratope plane. This would lead to a general guideline, as one would expect, to distribute the substitutions and avoid the CDRs in order to remediate the agitation-induced aggregation and retain the majority of biological activity.

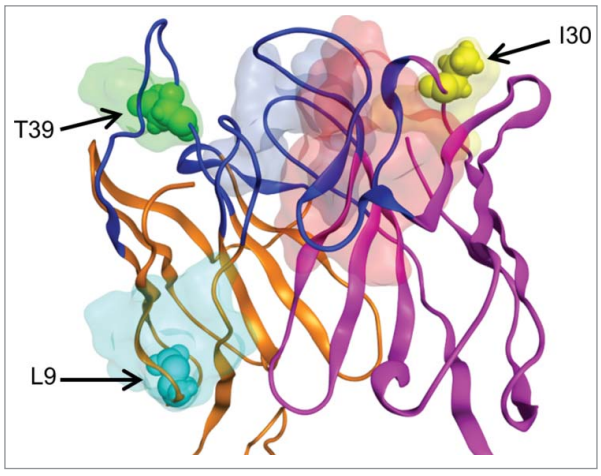

Figure 6. Location and type of mAb_A substitutions in variant 42. The 3 substitutions (T39D in green CPK, I30T in yellow CPK and L9D in aqua CPK) were effectively distributed on the Fv to remediate much of the aggregation experienced by the mAb_A parent. Their motifs are indicated by the translucent molecular surfaces. These 3 substitutions also caused minimal impact to biological activity as compared to the parent. The 2 large SAP motifs indicated by the red and blue molecular surfaces at the top-central region of the Fv conferred minimal instability on agitation in this construct.

Our rich data set has allowed us to explore interesting phenomena conferred by certain substitutions. An example follows describing an apparent binding mode switch between the antibody and the target. It is commonly thought that the major contributor to binding and activity of an antibody is the CDR_H3 loop, although we have found exceptions to this generality as have others.[21] Therefore, it would make sense to incorporate changes that introduce beneficial properties distant to CDR_H3 similar to the configuration of mAb_A_42. However, the next 2 most agitation stable and active antibodies included changes to W109 and W110, which were in CDR_H3 as defined by the Kabat CDR definition.[22] Although W109E and W110D were beneficial to agitation stability, these changes were also detrimental to bioactivity except in the presence of I30T_VH.

Tryptophan residues in CDR_H3 are often difficult to substitute without detriment to activity. This is probably due to their large size and formation of important hydrophobic contacts that are involved in intramolecular interactions within the CDR structure, as well as intermolecular interactions with the target. W109 and W110 were near the N-terminal end of the CDR_H3 loop and were 12% and 35% solvent exposed, respectively, as compared to the tripeptide 'AXA'. This calculated to 40 and 111

Table 3. Summary of variants with improved properties as compared to the mAb_A parent

	Stress Resistance Property		
	Agitation	**Thermal**	**Both**
Improved stability	47	39	32
Improved stability and binds target	20	13	11
Improved stability and biologically active	13	10	9

square angstroms of exposed surface area, respectively. This was sufficiently exposed to contribute to the designation of a large SAP motif. There was evidently enough exposed hydrophobicity for W109 and W110 to contribute to agitation instability as observed in the RAP assay since, when either W109E or W110D was included, most agitation stability of the variant was improved.

It is understood that the degree of freedom of CDR_H3 could also have increased exposed hydrophobicity during the RAP assay beyond what is observed in the mAb_A model. A molecular dynamics simulation might provide credence to this assertion to the significance of conformational mobility in the SAP calculation. Although variants with W109E and W110D were more agitation stable than the mAb_A parent, biological activity also decreased at least 50-fold in most of these variants. There were 2 exceptions, however. The only 2 variants with W109E and W110D that were active also had I30T_VH. All variants with isoleucine in position 30 of the VH were inactive when present with W109E and W110D. This could imply that a paratope/epitope interaction adjustment occurred from primarily a hydrophobic interaction to a hydrophilic, electrostatic interaction. The general guideline of avoiding substitutions within the CDR_H3 is probably reasonable. Unless information is known about the paratope/epitope interaction, it would be very difficult to rationally engineer a variant to the extent of predicting a situation as described above. Therefore, a large panel of engineered variants would be necessary to capture unexpected, functionally active candidates.

Many variants exhibited not only improved agitation stability, but also thermal stability. Chennamsetty et. al.[8] generated variants with improved thermal stability, although exposed hydrophobicity was the only biophysical criteria driving the engineering. In our work, the added thermal stability benefit did not always correlate with variants exhibiting improved agitation stability. Furthermore, there were no particular residues that always improved thermal stability. Improved thermal stability did not correlate with exposed hydrophobic surface area (data not shown) nor with the removal of non-germline residues. It has not been deduced why certain patterns of exposed hydrophobicity improve thermal stability while other patterns did not. However, some discrepancy between aggregation caused by thermal and agitation stress is certainly expected based on our previous work.[12] Temperature-induced aggregation reflects protein instability in bulk solutions, whereas agitation aggregation is triggered by denaturing events associated with exposure of protein to the air-water interface. To further isolate the effects of agitation on the protein, the agitation experiment is run under refrigerated conditions to minimize the influence of a potential thermal stress. Modeling indicated a large amount of surface hydrophobicity compared to surface hydrophilicity. The hydrophobicity will lead to preferentially consolidating the protein at the air-water interface.[23] This will increase local protein concentration at the air-water interface. If unfolding events also occur during this residency at the air-water interface, these 2 phenomena could be sufficient to drive aggregation. Adding charge residues may redirect aggregate formation to the bulk solution. Furthermore, increases in local concentration could have been prevented by repulsion of the appropriately distributed charged residues. Stabilization to thermal stress operates under a different mechanism possibly by increasing cooperativity of the folded structure, and thereby reducing its propensity to unfold. Substitution of hydrophobic surface residues could have induced beneficial intramolecular forces which improved thermal stability. The opposite effect of these agitation and thermal stresses on protein aggregation, including IgGs, has also been shown empirically with various protein concentrations[24] and excipients.[18,25-27]

Methods and Materials

Fab modeling

The parent Fv sequence of mAb_A was entered into the Antibody Modeler module within the Molecular Operating Environment (MOE, Chemical Computing Group, Montreal, CA). A template search for the homology modeling was performed using the PSILO database containing Amgen and public PDB structures. A highly homologous VL-VH framework pair was chosen followed by selection of appropriate loop segments for each of the CDRs. Energy minimization refinement with the Amber99 force field was used followed by GB/VI ranking to arrive at the working Fv model. To improve the quality of the Fv model, atom clashes, non-proline residues with cis peptides and any other non-ideality was manually corrected. Low-mode molecular dynamics of CDR3 of the VH was then performed to generate an ensemble of low energy conformations. The loop conformation with the lowest energy and absence of non-ideality, as listed above, was chosen.

To construct the Fab, appropriate constant domains with known structure were grafted onto the C-termini of the Fv. The modeled Fvs were superposed onto the Fvs of the Fab crystal structure to determine the proper Fv model domain/constant domain spatial relationship. The crystal structure Fvs were removed and the modeled Fvs were joined to the constant domains. Residues within 10 Å of the domain junction were energy minimized (Amber99). Assessment of the Fab for non-ideality (clashes, etc.) was performed and corrected if necessary.

Spatial aggregation propensity algorithm

The SAP algorithm as described in Chennamsetty et. al.[8] is shown below.

$$(SAP)_{atom\ i} = \sum_{\substack{Simulation \\ average}} \left\{ \sum_{\substack{Residues\ with \\ at\ least\ one \\ side\ chain\ atom \\ within\ R\ from\ atom\ i}} \left(\frac{\text{SAA of side chain atoms within radius R}}{\text{SAA of side chain atoms of fully exposed residue}} \right) \text{Residue Hydrophobicity} \right\}$$

Where *atom i* is every non-hydrogen atom in the structure, R is the radius, and SAA is the solvent accessible area. The radius used in our simulations was 5 Ångstroms. The residue hydrophobicity scale used was that published by Black and Mold[28] where Gly is assigned a value of 0. The degree of hydrophobicity is adjusted by the relationship of the SAA of the residue in context to the SAA of the fully exposed residue. The SAA of the fully exposed residue is defined as the degree of exposure of the interrogated residue in the fully extended conformation of the tripeptide Ala-X-Ala.

The Discovery Studio 3.5 suite of computational biology tools by Accelrys (San Diego, CA) utilizes this algorithm for calculating aggregation scores. The following procedure was used to determine the aggregation scores of Fab_A residues. The Fab_A . pdb structure generated by MOE was loaded into Discovery Studio and the Prepare Protein function was applied. This function confirmed that certain properties were addressed such as the presence of termini and the addition of missing atoms. The CHARMm force field was applied to complete the preparation of Fab_A. The Cutoff Radius parameter was set to 5 Å within the Calculate Aggregation Scores dialog. Default settings were used for all other parameters. The same Fab modeling procedure and SAP calculation method was used for Fab_B.

Fab engineering design

Sequence alignment and structure superposition was performed for Fab_A and Fab_B. Residues and motifs with high aggregation scores in Fab_A that had low scores in the corresponding positions in Fab_B were hypothesized to be relevant to differences in aggregation behavior between the 2 antibodies. The Amgen Reference numbering system was used, which within the Fv is based upon AHo numbering.[9] The rationale for using this numbering system is due to the association of sequence position with structural location. Therefore, sequence comparisons between the Fabs are directly relevant to antibody structural comparisons.

Nine sites were chosen in Fab_A for mutagenesis. Eight residues in Fab_A were changed to the corresponding positional residue in Fab_B. Of these 8 positions, 7 were modified in a combinatorial fashion. The eighth site (T39_VL) was substituted to aspartic acid in most designs. Since the ninth position was identical between Fab_A and Fab_B (I69_VH), this site was changed to residues with different chemical properties, either A, S, D, or K in isolation or in combination with all of the other 8 sites changed. The I69_VH central residue was a situation where it exhibited less solvent exposure and the local environment was chemically different in Fab_B as compared to Fab_A.

Using Fab_B as a guide for substitutions was not simply a matter of converting one Fab sequence to another since this would have resulted in too many combinations for the rational approach used here. Most of the 51 Fv positions that were different between Fab_A and Fab_B were not chemically similar. Therefore, the rational approach to understand the impact of each residue substitution would have been to generate constructs of every residue combination which would not have been practical. The SAP algorithm distilled down the potentially most relevant positions to 9. If Fab_B was not available as a guide for substitutions then each of the 9 sites could have been changed to a panel of residues. The panel would include residues that encompass the primary chemical amino acid properties (hydrophobicity, charge, etc.) such as Ala, Ser, Asp or Arg. Every combination would have been performed to understand the impact of each substitution on SAP motif calculation and aggregation propensity. This would have resulted in an untenable 262,144 variants. The strategy of using a somewhat homologous Fab and the SAP algorithm limited the number of variants to be made while still generating a rich data set to improve our understanding of engineering principles. Utilizing a closely related Fab also provides engineering direction to support our effort to maintain binding to the antibody target. **Table 2** outlines the engineering strategy of the mAb_A variants.

Antibody A IgG2 variant cloning

The parent mAb_A IgG2 in an appropriate mammalian transient transfection vector was used as a template to generate the engineered variant antibodies. The mutagenesis primers were designed using an in-house bioinformatics tool based upon the desired protein change. The primers were synthesized by Integrated DNA Technologies (Coralville, IA) and used with Agilent's (Santa Clara, CA) QuikChange II site-directed mutagenesis kit (part#200524) or Agilent's QuikChange Multi Site-Directed Mutagenesis Kit (part #200531). Top10 chemically competent *E. coli* cells by Invitrogen (Carlsbad, CA) were transformed as per manufacturer's recommendation, plated on Terrific Broth (Teknova, Hollister, CA) agar plates with carbenicillin (100 μg/mL) and grown overnight at 37°C. Resulting colonies were isolated and the plasmid DNA sequenced as

per manufacturer's guidelines on an Applied Biosystems (Foster City, CA) capillary sequencer. Desired constructs were grown overnight at 37°C in Terrific Broth media with carbenicillin (100 μg/mL) for plasmid purification. The plasmids were isolated using the Qiagen (Venlo, Limburg) 8000 liquid handling robot using their standard alkaline lysis, dual 96-well filter plate format.

IgG2 mammalian transient transfection and protein production

Expression constructs were transiently transfected using a slight variation of standard techniques.[29] 2936E Human Embryonic Kidney (HEK) cells stably expressing EBNA-1 (National Research Center of Canada) were cultured in suspension using 293 Freestyle media supplemented with 25 μg/mL Geneticin and 0.1% Pluronic F-68 obtained from Invitrogen (Carlsbad, CA). Transfection complexes were generated in 24-deep-well plates by adding 1 μg of DNA and 7 μg of a cationic polymer in 200 μL Freestyle media. Heavy chain and light chain plasmid DNA ratios were maintained at 1:1 normalized by mass and at 10% gene dosage. Gene dosage was achieved by compensating the coding DNA plasmids with 90% empty vector. The DNA/PEI mixture was allowed to incubate for 10 minutes at room temperature. For transfection, cells were directly dispensed to the 24-deep-well plate at 1×10^6 cells/mL for a final volume of 4 mL. Plates were shaken at 37°C and 5% CO_2 in a Kuhner (Basel, Switzerland) incubator with a shake speed of 240 RPM and orbital diameter of 25 mm. At one hour post transfection the wells received a feed of 0.5% yeastolate. Plates were placed on the shakers in the 37°C incubator and harvested 5 d post transfection.

Supernatant was isolated from the HEK cells by centrifugation at 1500 g for 5 minutes. The supernatant was removed for secretion titer measurement and protein enrichment. The human IgG2 concentration in the harvested culture media was quantitated using a Forte Bio Octet QKe (Menlo Park, CA) equipped with Protein A biosensors according to the manufacturer's instructions.

The IgG2 antibodies were one-step enriched by passing the supernatant through Phynexus Phytips (San Jose, CA) packed with Protein A affinity resin. The protocol followed was essentially as described by the manufacturer. After multiple IgG2 capture steps and 2 resin rinses, the protein was eluted with 100 mM acetic acid at pH 3.5 and neutralized with 1 M HEPES, pH 9.0 to a final pH of 6.0. On average, the amount of pure material produced for each construct was on the order of 20–40 μg at a concentration of 0.2–0.4 mg/mL.

IgG2 relative aggregation propensity assay

The RAP assay has been used to evaluate relative stability of mAb variants on a miniaturized scale to accommodate low production yields. The assay was performed on IgG mixtures subjected to either agitation (vortexing) or thermal stress, as previously described.[18,20] As this method depends on chromatographic resolution of different species for identification, all variants were analyzed individually before being assessed in mixtures. Then, 10 different mixtures of antibodies were prepared by selecting antibodies with non-overlapping CEX profiles. Each mixture was supplemented with several control IgGs of known stability (mAb-A, mAb-B or other) used as internal standards for assay performance. The RAP assay is sensitive to protein stability and can differentiate mAb molecules in various mixtures based on their propensity for forming aggregates. Protein monomers were separated from soluble and insoluble aggregates using cation-exchange chromatography (CEX; see below for method details), under non-denaturing conditions, and the individual components in the mixture were identified by retention time and quantitated relative to an unstressed control to obtain% monomer recovery. Agitation stress was induced by vigorous vortexing at 4°C in 100 mM sodium acetate, 50 mM sodium chloride at pH 5.2 (100A52N) at the maximal speed from a G-560 vortexer (Scientific Industries, Bohemia, NY). Two time points after 10 and 30 min of agitation were analyzed by removing small sample aliquots for CEX analysis. Thermal stress corresponded to a 10 minute incubation at 65°C on a Thermostat Plus heating block (Eppendorf 5352, Hamburg). Samples were briefly centrifuged prior to HPLC analysis to remove insoluble protein. The total protein material used for the RAP assay was ~10 μg of each individual mAb.

The CEX method[30] was run on an Agilent 1100 Series HPLC system using a ProPac WCX-10 analytical column (weak cation exchange, 4 × 250 mm; Dionex, Sunnyvale, CA) preceded by a ProPac WCX-10G guard column (weak cation exchange, 4 × 50 mm; Dionex) at ambient temperature and at a flow rate of 0.7 mL/min. The columns were equilibrated with Buffer A (20 mM sodium acetate, 0.0025% sodium azide, pH 5.2) and protein was eluted with a linear gradient of Buffer B (20 mM sodium acetate, 300 mM sodium chloride, 0.0025% sodium azide, pH 5.2) from 0 to 100% over 35 minutes. Following elution, the columns were washed with Buffer C (20 mM sodium acetate, 1 M sodium chloride, 0.0025% sodium azide, pH 5.2) for 5 minutes and re-equilibrated with Buffer A for 16 minutes. Chromatograms were analyzed with Dionex Chromeleon© software and the 280 nm signal was integrated to estimate protein peak area.

IgG2 affinity binding assay

Affinity binding experiments were performed using a Biacore T200 optical biosensor developed by Biacore AB (Uppsala, Sweden). Series S CM5 sensor chips, NaOH, coupling reagents (N-ethyl-N'-(3-dimethylaminopropyl)-carbodiimide hydrochloride (EDC)/ N-hydroxy-succinimide(NHS)), ethanolamine, acetate at pH 5.0 and glycine at pH 1.5 were purchased from GE Healthcare Biosciences (Piscataway, NJ). The hydrochloric acid (HCl) solution was purchased from Bio Rad Labs (Hercules, CA). HBS-EP buffer was purchased from Teknova (Hollister, CA). Goat anti-human IgG, Fcγ fragment specific was purchased from Jackson Immunoresearch (West Grove, PA).

Biosensor analysis was conducted at 25°C in HBS-EP running buffer (10 mM HEPES pH 7.4, 150 mM NaCl, 3.0 mM EDTA, 0.05% Polysorbate 20). The CM5 sensor chip was conditioned with 5, 30 second serial injections. The first 2 injections

were 0.1% SDS at a flow rate of 30 μL/min. The next 3 30 second serial injections were at a flow rate of 60 μl/min using 10 mM NaOH once, 10 mM HCl once and finally with 0.1% SDS. Goat anti-human IgG, Fcγ fragment-specific was prepared in 10 mM sodium acetate, pH 5.0, at a concentration of 15 μg/mL and immobilized to the sensor chip via standard amine coupling (EDC/NHS) and ethanolamine blocking to flow cells 1–4.[31] 5 μL antibody injections at a concentration of 5 μg/mL were performed in sets of 3 over either flow cell 2, 3 or 4 at a flow rate of 10 μl/min. This captured on average around 100 resonance units of antibody. After the capture step, 25 nM antigen was passed over flow cells 1–4 at a flow rate of 50 μL/min to observe the association to each antibody over an 180 second duration. Each flow cell was then flushed with running buffer to observe the dissociation of antigen from the chip surface over a 180 second duration. Blank injections were run before each set of 3 antibodies to determine the baseline of each flow cell. The surface was regenerated with 15 μL of 10 mM Glycine-HCL, pH 1.5, at a flow rate of 50 μL/min. The data was analyzed with Biacore T200 Evaluation Software Version 1.0 (General Electric Company) as follows. Data from flow cell 1 (blank reference) was subtracted from the data from flow cells 2–4 (assay flow cells). This reference subtracted data was then subtracted (double referenced) from the corresponding blank injections of each flow cell. The dissociation rate constant (k_d) was fit to a 1:1 binding model and used as a fixed parameter to determine the association rate constant (k_a). The equilibrium dissociation constant (K_d) was determined from the following equation: $K_d = k_d/k_a$.

IgG2 natural killer assay

Primary human natural killer (NK) cells were isolated from leukophoresis products obtained from Puget Sound Blood Center and frozen at −80°C into aliquots of 20×10^6 cells per vial. RPMI 1640 media and supplements were purchased from Invitrogen (Carlsbad, CA). Recombinant human IL-12 and IFN-γ ELISA Duo Set (cat# DY285) was purchased from R & D Systems (Minneapolis, MN). The rhIL-33 was generated at Amgen (Seattle, Washington).

Frozen primary NK cells were thawed in pre-warmed Immune Cell Media (RPMI 1640, 10% heat inactivated FBS, 5 mM L-glutamine, 1× sodium pyruvate, 20 mM HEPES, 55 μM 2-Mercaptoethanol), washed twice and diluted to 1×10^6 cell per mL. NK cells were seeded at 5×10^4 cells per well in a 96-well round bottom plate in 50 μl Immune Cell Media (ICM). Investigated antibodies or control antibody titrations were prepared at 4× final concentration, covering a range of 3.3 nM to 0.21 pM in ICM. NK cells were pre-treated for 30 minutes at 37°C, 5% CO_2 with the addition of 25 μL of each antibody titration. Cells were stimulated with the addition of 25 uL human IL-33 (55 pM final) + recombinant human IL-12 (1.7 nM final) prepared in ICM. An unstimulated control was also included on each plate containing rhIL-12 only. Supernatants were collected after 48 hrs of incubation at 37°C, 5% CO_2 and analyzed for IFN-γ release by IFN-γ ELISA as per manufacturer's instructions. Fluorescence absorbance was measured with a Tecan GENios Pro instrument. Percent inhibition was calculated in the following manner:

$$\{(\text{IFN}-\gamma \text{ calculated concentration of treated sample}) - (\text{unstimulated control})\}/\{(\text{the calculated average IFN}-\gamma \text{ concentration of untreated cells}) - (\text{unstimulated control})\}.$$

Disclosure of Potential Conflicts of Interest

No potential conflicts of interest were disclosed.

References

1. Maggon K. Monoclonal antibody "Gold Rush". Curr Med Chem 2011; 14:1978-87; http://dx.doi.org/10.2174/092986707781368504
2. Vázquez-Rey M, Lang DA. Aggregates in monoclonal antibody manufacturing processes. Biotechnol Bioeng 2011; 108:1494-508; http://dx.doi.org/10.1002/bit.23155
3. Cromwell MEM, Hilario E, Jacobson F. Protein aggregation and bioprocessing. AAPS J 2006; 8:E572-9; PMID:17025275; http://dx.doi.org/10.1208/aapsj080366
4. Cordoba-Rodriguez RV. Aggregates in MAbs and recombinant therapeutic proteins: a regulatory perspective. BioPharm Int 2008; 21
5. Hermeling S, Crommelin DJ a, Schellekens H, Jiskoot W. Structure-immunogenicity relationships of therapeutic proteins. Pharm Res 2004; 21:897-903; PMID:15212151; http://dx.doi.org/10.1023/B:PHAM.0000029275.41323.a6
6. Chi EY, Krishnan S, Randolph TW, Carpenter JF. Physical stability of proteins in aqueous solution: mechanism and driving forces in nonnative protein aggregation. Pharm Res 2003; 20:1325-36; PMID:14567625; http://dx.doi.org/10.1023/A:1025771421906
7. Ó'Fágáin C. Engineering protein stability. In: Walls D, Loughran ST, eds. Protein Chromatography. Springer: New York Dordrecht Heidelberg London; 2011; 103-36
8. Chennamsetty N, Voynov V, Kayser V, Helk B, Trout BL. Design of therapeutic proteins with enhanced stability. Proc Natl Acad Sci U S A 2009; 106:11937-42; PMID:19571001; http://dx.doi.org/10.1073/pnas.0904191106
9. Honegger A, Plückthun A. Yet another numbering scheme for immunoglobulin variable domains: an automatic modeling and analysis tool. J Mol Biol 2001 309:657-70; PMID:11397087; http://dx.doi.org/10.1006/jmbi.2001.4662
10. Perchiacca JM, Ladiwala ARA, Bhattacharya M, Tessier PM. Aggregation-resistant domain antibodies engineered with charged mutations near the edges of the complementarity-determining regions. Protein Eng Des Sel 2012 25:591-601; PMID:22843678; http://dx.doi.org/10.1093/protein/gzs042
11. Kwon WS, Da Silva NA, Kellis JT. Relationship between thermal stability, degradation rate and expression yield of barnase variants in the periplasm of Escherichia coli. Protein Eng 1996; 9:1197-202; PMID:9010933; http://dx.doi.org/10.1093/protein/9.12.1197
12. Buchanan A, Clementel V, Woods R, Harn N, Bowen MA, Mo W, Popovic B, Bishop SM, Dall'Acqua W, Minter R, et al. Engineering a therapeutic IgG molecule to address cysteinylation, aggregation and enhance thermal stability and expression. MAbs 2013; 5:255-62; PMID:23412563; http://dx.doi.org/10.4161/mabs.23392
13. Schaefer JV, Plückthun A. Transfer of engineered biophysical properties between different antibody formats and expression systems. Protein Eng Des Sel 2012; 25:485-506; PMID:22763265; http://dx.doi.org/10.1093/protein/gzs039
14. Pezzullo M, Del Vecchio P, Mandrich L, Nucci R, Rossi M, Manco G. Comprehensive analysis of surface charged residues involved in thermal stability in Alicyclobacillus acidocaldarius esterase 2. Protein Eng Des Sel 2013; 26:47-58; PMID:23035254; http://dx.doi.org/10.1093/protein/gzs066
15. Selkoe DJ. Folding proteins in fatal ways. Nature 2003; 426:900-4; PMID:14685251; http://dx.doi.org/10.1038/nature02264
16. Pace CN, Shirley BA, Mcnutt M, Gajiwala K. Forces contributing to the conformational stability of proteins. FASEB J 1996; 10:75-83; PMID:8566551
17. Agrawal NJ, Kumar S, Wang X, Helk B, Singh SK, Trout BL. Aggregation in protein-based biotherapeutics : computational studies and tools to identify aggregation-prone regions. Pharm Res 2011; 100:5081-95
18. Chen S, Lau H, Brodsky Y, Kleemann GR, Latypov RF. The use of native cation-exchange chromatography to study aggregation and phase separation of monoclonal antibodies. Protein Sci 2010 19:1191-204; PMID:20512972; http://dx.doi.org/10.1002/pro.396
19. Hari SB, Lau H, Razinkov VI, Chen S, Latypov RF. Acid-induced aggregation of human monoclonal IgG1 and IgG2: molecular mechanism and the effect of solution composition. Biochemistry 2010 49:9328-38; PMID:20843079; http://dx.doi.org/10.1021/bi100841u
20. Woodard J, Lau H, Latypov RF. Nondenaturing size-exclusion chromatography-mass spectrometry to

measure stress-induced aggregation in a complex mixture of monoclonal antibodies. Anal Chem 2013; 85:6429-36; PMID:23742703; http://dx.doi.org/10.1021/ac401455f
21. Burkovitz A, Leiderman O, Sela-Culang I, Byk G, Ofran Y. Computational identification of antigen-binding antibody fragments. J Immunol 2013 190:2327-34; PMID:23359499; http://dx.doi.org/10.4049/jimmunol.1200757
22. Kabat EA, Wu TT, Perry HM, Gottesman KS, Foeller C. Sequences of Proteins of Immunological Interes. Darby, PA: DIANE Publishing; 1992
23. Baszkin A, Boissonnade M, Kamyshny A, Magdassi S. Native and hydrophobically modified human immunoglobulin G at the Air/Water interface. J Colloid Interface Sci 2001; 239:1-9; PMID:11397041; http://dx.doi.org/10.1006/jcis.2001.7521
24. Treuheit MJ, Kosky AA, Brems DN. Inverse relationship of protein concentration and aggregation. Pharm Res 2002; 19:511-6; PMID:12033388; http://dx.doi.org/10.1023/A:1015108115452
25. Thirumangalathu R, Krishnan S, Ricci MS, Brems DN, Randolph TW, Carpenter JF. NIH public access. J Pharm Sci 2009; 98:3167-81; PMID:19360857; http://dx.doi.org/10.1002/jps.21719
26. Abbas SA, Sharma VK, Patapoff TW, Kalonia DS. Opposite effects of polyols on antibody aggregation: thermal versus mechanical stresses. Pharm Res 2012 29:683-94; PMID:21948456; http://dx.doi.org/10.1007/s11095-011-0593-4
27. Liu L, Qi W, Schwartz DK, Randolph TW, Carpenter JF. The effects of excipients on protein aggregation during agitation : an interfacial shear rheology study. J Pharm Sci 2013; 102:2460-70; PMID:23712900; http://dx.doi.org/10.1002/jps.23622
28. Black SD, Mould DR. Development of hydrophobicity parameters to analyze proteins which bear post- or cotranslational modifications. Anal Biochem 1991; 193:72-82; PMID:2042744; http://dx.doi.org/10.1016/0003-2697(91)90045-U
29. Zhang J, Liu X, Bell A, To R, Baral T, Azizi A, Li J, Cass B, Durocher Y. Transient expression and purification of chimeric heavy chain antibodies. Protein Expr Purif 2009; 65:77-82; PMID:19007889; http://dx.doi.org/10.1016/j.pep.2008.10.011
30. Lau H, Pace D, Yan B, McGrath T, Smallwood S, Patel K, Park J, Park SS, Latypov RF. Investigation of degradation processes in IgG1 monoclonal antibodies by limited proteolysis coupled with weak cation-exchange HPLC. J Chromatogr B Analyt Technol Biomed Life Sci 2010 878:868-76; PMID:20206584; http://dx.doi.org/10.1016/j.jchromb.2010.02.003
31. Johnsson B, Lofas S, Lindquist G. Immobilization of proteins to a carboxymethyldextran-modified gold surface for biospecific interaction analysis in surface plasmon resonance sensors. Anal Biochem 1991; 198:268-77; PMID:1724720; http://dx.doi.org/10.1016/0003-2697(91)90424-R